JOURNAL OF OPTOELECTRONICS AND ADVANCED MATERIALS Vol. 12, No. 3, March 2010, p. 547 - 552

Patterning and annealing of nanocrystalline $LiCoO_2$ thin films

R. KOHLER*, P. SMYREK, S. ULRICH, M. BRUNS[a], V. TROUILLET[a], W. PFLEGING
Institute for Materials Research (IMF-I), Karlsruhe Institute of Technology (KIT), P.O. Box 3640 Karlsruhe, Germany
[a]Institute for Materials Research (IMF-III), Karlsruhe Institute of Technology (KIT), P.O. Box 3640 Karlsruhe, Germany

For the development of new high power density cathode materials for lithium ion batteries (LIB) the combination of thin film technology and laser technology is investigated. For this purpose thin films of lithium cobalt oxide ($LiCoO_2$) synthesized by r.f. magnetron sputtering were structured with laser radiation to significantly increase the active surface area. Subsequent heat treatment using laser annealing was performed in order to synthesize the required high temperature phase of $LiCoO_2$. The cathode material was studied by Raman spectroscopy to determine the structure before and after laser treatment. X-ray photoelectron spectroscopy was applied to determine the chemical composition of the films. The battery performance of laser treated cathode material was investigated by means of electrochemical cycling. A significant improvement of capacity retention by laser structuring was detected.

(Received June 21, 2009; accepted October 23, 2009)

Keywords: Lithium ion batteries, Laser structuring, Laser annealing, Thin film technology, $LiCoO_2$

1. Introduction

Development of lithium ion batteries (LIB) has gained an unprecedented significance in the last two decades as the demand for portable telecommunication devices, computers and hybrid electric vehicles as well as full electric vehicles has been steadily increasing [1]. Because of their high energy density LIB have become desirable energy storage devices for a diverse group of portable applications. Thin film LIB are especially desired for their small dimensions, making them suitable for micro-electric systems. Additionally, their large surface area may allow high current rates making them applicable for high power devices.

The development of new cathode materials has attracted a great deal of attention and although other materials show very good potential, lithium cobalt oxide ($LiCoO_2$) is still most commonly used as cathode material in lithium ion batteries [2].

For the preparation of $LiCoO_2$ thin films, different methods, including pulsed laser deposition [3,4], chemical vapor deposition [5,6], sol-gel spin coating [7,8], as well as r.f. magnetron sputtering [9,10], have been applied. Yet commonly a post annealing process is necessary to create the high temperature phase of $LiCoO_2$ (HT-$LiCoO_2$), which exhibits a high specific energy density of about 140 mAh/g and good capacity retention.

Previous work has shown, that thin films deposition via r.f. magnetron sputtering in 10 Pa argon atmosphere using a stoichiometric $LiCoO_2$ target leads to nearly stoichiometric films of $LiCoO_2$ [9]. A new technical approach is to significantly increase the surface area of thin films through laser structuring [9,11]. Also, for the subsequent annealing procedure the use of laser annealing will be investigated.

2. Experimental

2.1 Thin film deposition and furnace annealing

The thin film cathodes were deposited using a Leybold Z550 coating facility by non-reactive r.f. magnetron sputtering in pure argon plasma. The target power was 200 W and the argon gas pressure was adjusted to 10 Pa. A detailed description of the coating facility and the dependence of the processing parameters can be found in [12]. Due to heating from the plasma processes, the substrate temperature can be estimated between 80 °C and 100 °C.

Furnace annealing of the thin film cathodes took place for 3 hours in an argon-oxygen atmosphere (20 % argon) of 10 Pa at temperatures between 400 °C and 600 °C. A heating and cooling ratio of $\Delta T/\Delta t = 300°C/h$ was used.

2.2 Laser technology

Laser material processing was applied for highly selective surface structuring and crystalline modification of thin films made of $LiCoO_2$. For this purpose micro-structuring via ablation and laser-assisted annealing were investigated.

Laser structuring was performed with ATLEX-500-SI and ATLEX-300-M (ATL Lasertechnik GmbH) short pulse excimer laser radiation with wavelengths of 248 nm and 193 nm and laser pulse lengths of 4 - 6 ns (FWHM). The short pulse excimer lasers generate a raw “flat-top” beam directly applicable without homogenizing devices for various micro-processing applications [13].

For laser annealing a high power diode laser (FLS IronScan, Fisba Optik AG) with a maximum laser output power of 50 W and a wavelength of 940 nm was used. The

laser beam has a focus diameter of about 1 mm on the sample surface. The temperature in the heat-affected-zone is measured on-line during the annealing process with a pyrometer (FLS PyroS, Fisba Optik AG) that is linked with the laser power management system. The process temperature can be controlled in the range of 120 °C up to 700 °C. Laser annealing of cathode materials (1.5 x 5 mm^2) was performed in ambient air for 13.2 s.

2.3 Analytics

Structural information on the $LiCoO_2$ coatings was obtained by micro-Raman spectroscopy at room temperature using a Renishaw-1000 system equipped with an argon ion laser (excitation wavelength λ_{Raman} = 514.5 nm, power output 21 mW).

X-ray photoelectron spectroscopy (XPS) measurements were performed in a K-Alpha XPS spectrometer (ThermoFisher Scientific, East Grinstead, UK). Data acquisition and processing using the Thermo Avantage software is described elsewhere [14]. All thin films were analyzed using a microfocused, monochromatic Al Kα X-ray source (30-400 µm spot size). The spectra were fitted with one or more Voigt profiles and Scofield sensitivity factors were applied for quantification [15]. All spectra were referenced to the C1s peak assumed to originate from surface hydrocarbon contamination at 285.0 eV binding energy, and to the Au $4f_{7/2}$ peak at 84.0 eV, respectively.

Electrochemical characterisation was performed in CR2023 type button cells with a Princeton Applied Research / BioLogic VMP3 potentiostat/galvanostat. Metallic lithium was used as anode material with conventional EC/EDC electrolyte containing 1M $LiPF_6$. Battery cycling was performed at a constant current between 3.0 V and 4.2 V. The theoretical capacity in this voltage range of 140 mAh/g was used for the calculation of the C-rate. The C-rate is a measure of the rate at which a battery is charged / discharged relative to its maximum capacity. A "1C" rate means that the discharge current will discharge the entire battery in 1 hour.

3. Results and discussion

3.1 Laser structuring

One objective of this work is to increase the active surface area of thin film cathodes by means of laser structuring, therefore two approaches may be suitable. One is to induce specific surface structures, e.g. by mask imaging, and the other is to perform laser structuring close to the ablation threshold in order to change the surface topography by selective material ablation.

For $LiCoO_2$ thin films deposited by r.f. magnetron sputtering the formation of conical surface structures could be observed within a wide laser fluence range [11]. Also, with laser fluences above 2 J/cm² the creation of smooth surfaces was possible. It could also be observed, that a large amount of ablated material was re-deposited on the surface not only on the side of the laser structured area, but also on the ablated surface itself, leading to an increasing height of the conical surface structures (Fig. 1). On 3 µm thick thin film, structures with a height of > 5 µm up to 8µm could be produced, leading to a surface area which is estimated to be 5 to 10 times larger than the as-deposited layer. Because of the re-deposition process the total amount of active material was only slightly reduced, a material loss of smaller than 15 % can be estimated.

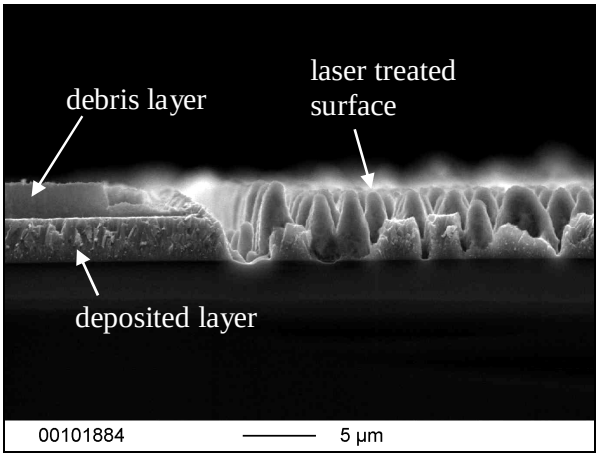

Fig. 1. SEM image of a cross-section of laser structured $LiCoO_2$ thin film deposited on a silicon substrate (wavelength λ = 248 nm, laser fluence ε = 1.0 J/cm², repetition rate ν_{rep} = 100 Hz, laser pulse number n = 50, processing gas: helium, substrate: silicon).

The formation of conical surface structures can be observed in a variety of different materials, e.g. stainless steel [16], silicon [17] or polymers [18] with laser wavelengths ranging from the UV to the IR. Different possible mechanisms leading to their creation have been discussed. One is that melt transfer occurs along the surface of the irradiated structures from liquid flow driven by surface tension gradients. Since with most materials the surface tension decreases with rising temperature, the material is transported from warmer regions to colder regions leading to growth of surface structures [16]. If a dry-etching process is dominant during ablation, the cone growth can be attributed to redeposited ablation particles. In case of polymers a shielding of the surface structures by either impurities or redeposited carbon is proposed [18]. Since a large amount of redeposited material is encountered (cf. Fig. 1) the latter model seems more plausible. It is assumed, that the morphological structure of the thin films strongly influences the cone formation and cone size. The conical surface structures, as shown in Fig. 2, could be created by using laser ablation either in the step-and-repeat mode or by using the scanning mode with a specific speed and laser repetition rate resulting in a defined pulse overlap:

$$\text{pulse overlap} = \frac{\text{lateral mask size}}{\text{laser pulse number}} \qquad (1)$$

Scanning over the surface led to the formation of periodic surface structures, when specific mask sizes and laser repetition rates were used. Fig. 2 shows two $LiCoO_2$ thin film surfaces, which were laser structured with identical laser parameters but with different operation mode (step-and-repeat versus scanning mode). While the cones are randomly distributed with scanning mode, a periodical arrangement of conical surface structures oriented perpendicular to the scanning direction can be found working in step-and-repeat mode.

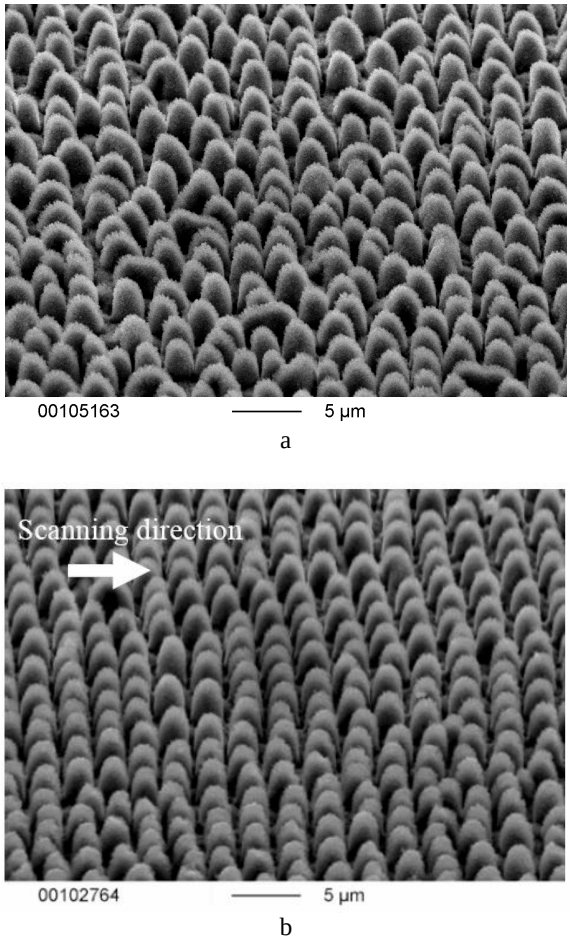

Fig. 2. SEM images of $LiCoO_2$ thin films laser structured by step-and-repeat mode (a) and by scanning mode (b) (wavelength λ = 193 nm, fluence ε = 1.0 J/cm², repetition rate ν_{rep} = 100 Hz, pulse number n = 40, processing gas: helium, pulse overlap p = 2.5 µm, substrate: silicon).

As different pulse overlaps yielded different structures a close correlation between the periodicity of the surface structures and the laser pulse overlap could be found. The periodical surface structures encountered, had a periodicity of 2.5 µm to 5 µm, witch matched the pulse overlap precisely. It can therefore be concluded that the periodicity is a direct result of the laser scan overlap.

3.2 Laser annealing

Laser annealing was applied to the thin films to create HT-$LiCoO_2$. The Raman spectra of $LiCoO_2$ thin films laser annealed at different temperatures are shown in

Fig. *3*. The as-deposited layer shows two broad peaks at 510 cm^{-1} and 600 cm^{-1}. After annealing at 400 °C the two peaks have shifted to 482 cm^{-1} and 695 cm^{-1} which can be attributed to HT-$LiCoO_2$ [19]. With higher temperatures the intensity and the sharpness of the peaks increases.

At wave numbers between 650 cm^{-1} and 700 cm^{-1} there is also a relatively small, broad peak visible. This can be induced by either CoO or Co_3O_4 with show spectra at 668 cm^{-1} and 691 cm^{-1}, respectively, and can be an indication of a slight lithium deficiency [17].

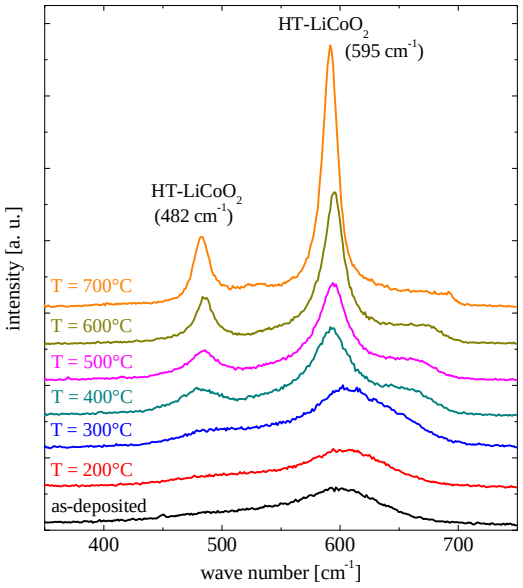

Fig. 3. Raman spectra of laser annealed $LiCoO_2$ thin films at different temperatures.

The crystallization seems to be to be highest at 700 °C, since the FWHM is lowest. Nevertheless, an additional important criterion is the grain size of $LiCoO_2$ which has to be as small as possible in order to improve battery performance [18]. While the average grain size of the as-deposited layer, as shown in Fig. 4 (left), is about 50 nm, the grain size after laser annealing at 600 °C has increased up to 100 nm (Fig. 4, middle), reaching a crystallite size of > 1 µm after annealing at 700 °C.

The formation of cracks was also observed after the laser annealing process. While the crack size stayed below 200 nm for thin films annealed at 600 °C, crack widths larger than 1 µm could be obtained after annealing at 700 °C. Yet, no delamination of the thin film was encountered after laser annealing.

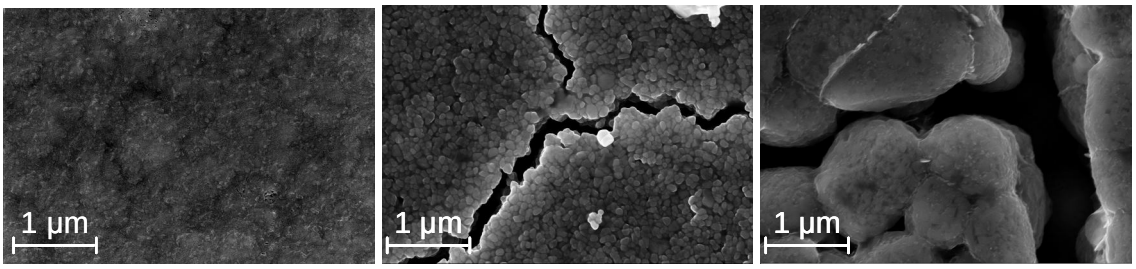

Fig. 4. Surface SEM images of $LiCoO_2$ thin films, as-deposited (left), laser annealed at 600 °C (middle) and 700 °C (right) (substrate: stainless steel).

Compared to conventional furnace annealing a large decrease of processing time using laser annealing is possible, resulting from the low heating and cooling rates. Additionally opposite to furnace annealing no delamination was encountered. Other annealing techniques have also been applied to $LiCoO_2$, e.g. rapid thermal annealing (RTA) [20-22]. One of the main differences between RTA and laser annealing is the heat source, while RTA uses mainly incoherent halogen lamps laser annealing utilizes focused laser radiation. Therefore, contrary to RTA, laser annealing can be applied locally and is scanned over the surface for large area applications. Additionally, the optical absorption coefficient at 940 nm was measured to $\alpha = 0.5\ \mu m^{-1}$, which means the laser power is absorbed in the first two micron of the surface. Therefore the laser beam effectively heats up the thin film volume.

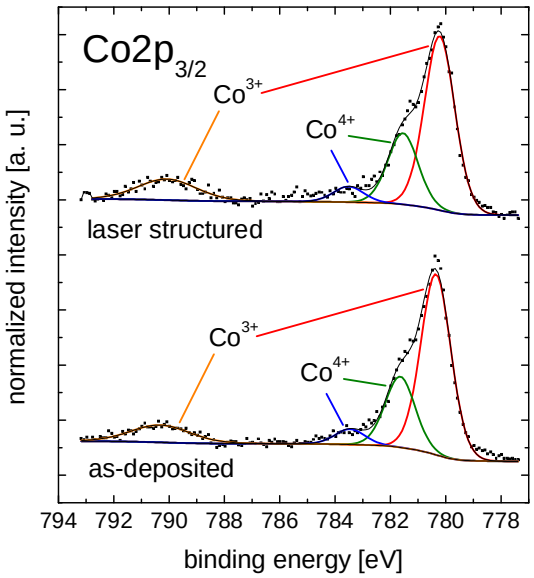

Fig. 5. XPS spectra of $Co2p_{3/2}$-peaks with their associated shake-up satellites of untreated (bottom) and structured (top) $LiCoO_2$ thin films (wavelength $\lambda = 248$ nm, laser fluence $\varepsilon = 1.9$ J/cm², repetition rate $\nu_{rep} = 100$ Hz, pulse number $n = 50$, processing gas: helium, laser annealing at $T = 600$°C).

To further investigate the laser-induced chemical changes at the surface, XPS measurements of laser structured and unstructured thin films, which were laser annealed at 600 °C, were performed. For this purpose the line shape of the $Co2p_{3/2}$-peak was studied in detail (Fig. 5). The associated shake-up satellite structures are typical and well known from literature [23]. The main photoelectron peak is, as expected, from Co^{3+} in $LiCoO_2$. The formation of Co^{4+} was also observed. The occurrence of Co^{4+} can be explained by an excess of oxygen [24]. The surface chemistry of the redeposited material after laser structuring is unchanged compared to the unstructured thin film. This was also verified by XPS depth profiling within a depth of 100 nm.

3.3 Battery cycling

Battery cycling was carried out to determine the influence of laser structuring on the electrochemical performance of the cathode material. After 30 cycles at C/20 the charge/discharge current was increased to C/4 and after another 30 cycles the batteries were cycled over 300 times at 1.25·C (Fig. 6). In all cases the thin films that were laser structured with 248 nm laser wavelength showed the highest capacity. A drop of discharge capacity after each increase of charging current was visible. Yet, the amount of capacity loss strongly depended on the production process. The capacity of the unstructured films dropped by 37 % after the five-fold increase of charging current from C/20, while the structured films dropped by 22.5 % and 15 %, respectively. When raising the charging current to 1.25·C the capacity decreased by 68 % (unstructured), 31 % (193 nm) and 24.5 % (248 nm). During cycling at the highest electrical current the unstructured film lost almost 90 % of its capacity, while the structured films retained 61 % (193 nm) and 53 % (248 nm).

The improvement of battery performance by laser structuring can be attributed to different processes. First of all the free standing cones contain little residual stress, also expansion during electrochemical cycling can be easily compensated, leading to reduced crack formation. Through the increased surface area of the structured films more lithium diffusion plains are accessible which in turns leads to an increased lithium diffusion and an improved performance at high charging rates.

Since the ablation rate with laser radiation at a wavelength of 248 nm is higher than with 193 nm [11] the height of the cones using 248 nm is increased. This is the probable cause for the better performance of the thin films structured with the KrF excimer laser radiation.

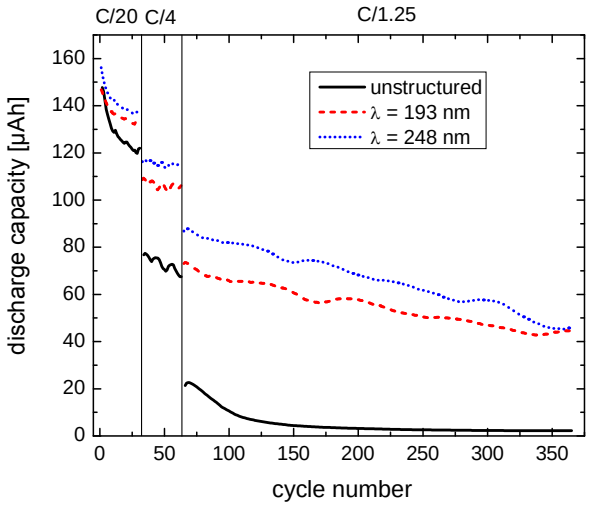

Fig. 6. Discharge capacity as a function of the cycle number of unstructured and laser structured $LiCoO_2$ thin films after furnace annealing at 400°C. Laser structuring was performed with wavelengths λ = 193 nm (laser fluence ε = 1.0 J/cm², repetition rate ν_{rep} = 200 Hz, pulse number n = 40) and λ = 248 nm (ε = 1.0 J/cm², ν_{rep} = 300 Hz, n = 50) in helium atmosphere.

4. Summary and outlook

Laser structuring of $LiCoO_2$ thin films with a thickness of 3 µm was performed and an increase of active surface area of 5 up to 10 could be obtained. By applying the laser scanning mode conical surface structures could be aligned periodically. A direct correlation between the pulse overlap and the periodicity was detected.

Battery cycling showed a significant improvement of capacity retention and cycle stability especially at large C-rates.

Laser annealing resulted in the formation of HT-$LiCoO_2$ with low content of impurity shown by Raman spectroscopy and XPS. The grain size of the cathode material can be adjusted from the nm-range up to the µm-scale as function of annealing temperature.

Future experimental studies will be focused on the optimization of annealing time and temperature with respect to crystallinity, grain size and mechanical stability. Also the influence of different processing gases and structure geometries will be studied and verified by battery cycling.

Acknowledgements

We are grateful to U. Geckle and M. Beiser for their technical assistance in SEM. We are indebted to H. Besser for his support in laser material processing. We also want thank S. Zils and A. Knorr for the r.f. sputtering of the thin films. For helpful discussion and assistance in electrochemical measurements we want to thank S. Indris. We gratefully acknowledge the financial support by the program NANOMIKRO of the Helmholtz association.

References

[1] A. Patil, V. Patil, D. Wook Shin, J.-W. Choi, D.-S. Paik,S.-J. Yoon, **43**, 1913 (2008)
[2] Y. Zhang, C. Chung and M. Zhu, **27**, 266 (2008).
[3] S.B. Tang, M.O. Lai and L. Lu, J. Alloy. Compd. **424**, 342 (2006).
[4] H. Xia, L. Lu, Electrochim. Acta **52**, 7014 (2007).
[5] S.-I. Cho, S.-G. Yoon, J. Electrochem. Soc. **149**, A1584 (2002).
[6] J.F.M. Oudenhoven, T. van Dongen, R.A.H. Niessen, M. de Croon, P.H.L. Notten, J. Electrochem. Soc. **156**, D169 (2009) .
[7] T. Matsushita, K. Dokko, K. Kanamura, J. Electrochem. Soc. **152**, A2229 (2005).
[8] K.W. Kim, S.I. Woo, K.H. Choi, K.S. Han and Y.J. Park, Solid State Ionics **159**, 25 (2003) .
[9] B. Ketterer, H. Vasilchina, K. Seemann, S. Ulrich, H. Besser, W. Pfleging, T. Kaiser, C. Adelhelm, Int. J. Mater. Res. **99**, 1171 (2008).
[10] H. Pan and Y. Yang, **189**, 633 (2009).
[11] R. Kohler, J. Proell, S. Ulrich, V. Trouillet, S. Indris, M. Przybylski and W. Pfleging, in W. Pfleging, Y. Lu, K. Washio, W. Hoving and J. Amako (Eds.), Proceedings of the SPIE, 7202, 2009, p. 720207-720207-11.
[12] A. Kratzsch, S. Ulrich, H. Leiste, M. Stuber and H. Holleck, Surf. Coat. Tech. **119**, 949 (1999) -955.
[13] W. Pfleging and O. Baldus, in F. G. Bachmann, W. Hoving, Y. Lu and K. Washio (Eds.), Proceedings of SPIE, 6107, 2006, p.
[14] K.L. Parry, A.G. Shard, R.D. Short, R.G. White, J.D. Whittle, A. Wright, Surf. Interface Anal. **38**, 1497 (2006).
[15] J.H. Scofield, J. Electron. Spectrosc. Relat. Phenom. **8**, 129 (1976).
[16] R. Lloyd, A. Abdolvand, M. Schmidt, P. Crouse, D. Whitehead, Z. Liu and L. Li, Appl. Phys. A-Mater. Sci. Process. **93**, 117 (2008).
[17] S.I. Dolgaev, S.V. Lavrishev, A.A. Lyalin, A. Simakin, V.V. Voronov and G.A. Shafeev, Appl. Phys. A-Mater. Sci. Process. **73**, 177 (2001).
[18] V. Oliveira and R. Vilar, Appl. Phys. A-Mater. Sci. Process. **92,** 957 (2008) .

[19] M. Inaba, Y. Iriyama, Z. Ogumi, Y. Todzuka and A. Tasaka, J Raman Spectrosc **28**, 613 (1997).
[20] H.K. Kim and Y.S. Yoon, J. Vac. Sci. Technol. A **22**, 1182 (2004).
[21] H.Y. Park, S.C. Nam, Y.C. Lim, K.G. Choi, K.C. Lee, G.B. Park, J.B. Kim, H.P. Kim, S.B. Cho, Electrochim. Acta **52**, 2062 (2007).
[22] M. Okubo, E. Hosono, T. Kudo, H.S. Zhou, I. Honma, Solid State Ionics **180**, 612 (2009).
[23] D. Ensling, A. Thissen, Y. Gassenbauer, A. Klein and W. Jaegermann, Adv. Eng. Mater. **7**, 945 (2005).
[24] J.C. Dupin, D. Gonbeau, H. Benqlilou-Moudden, P. Vinatier and A. Levasseur, Thin Solid Films **384**, 23 (2001).

*Corresponding author: robert.kohler@imf.fzk.de